PROTEINS
STRUCTURE ■ FUNCTION ■ BIOINFORMATICS

All-atom structural models of insulin binding to the insulin receptor in the presence of a tandem hormone-binding element

Harish Vashisth[1]* and Cameron F. Abrams[2]

[1] Department of Chemistry and Biophysics Program, University of Michigan, Ann Arbor, Michigan

[2] Department of Chemical and Biological Engineering, Drexel University, Philadelphia, Pennsylvania

ABSTRACT

Insulin regulates blood glucose levels in higher organisms by binding to and activating insulin receptor (IR), a constitutively homodimeric glycoprotein of the receptor tyrosine kinase (RTK) superfamily. Therapeutic efforts in treating diabetes have been significantly impeded by the absence of structural information on the activated form of the insulin/IR complex. Mutagenesis and photo-crosslinking experiments and structural information on insulin and apo-IR strongly suggest that the dual-chain insulin molecule, unlike the related single-chain insulin-like growth factors, binds to IR in a very different conformation than what is displayed in storage forms of the hormone. In particular, hydrophobic residues buried in the core of the folded insulin molecule engage the receptor. There is also the possibility of plasticity in the receptor structure based on these data, which may in part be due to rearrangement of the so-called CT-peptide, a tandem hormone-binding element of IR. These possibilities provide opportunity for large-scale molecular modeling to contribute to our understanding of this system. Using various atomistic simulation approaches, we have constructed all-atom structural models of hormone/receptor complexes in the presence of CT in its crystallographic position and a thermodynamically favorable displaced position. In the "displaced-CT" complex, many more insulin–receptor contacts suggested by experiments are satisfied, and our simulations also suggest that R-insulin potentially represents the receptor-bound form of hormone. The results presented in this work have further implications for the design of receptor-specific agonists/antagonists.

Proteins 2013; 81:1017–1030.

Key words: insulin receptor; diabetes; temperature-accelerated molecular dynamics; string method; Monte-Carlo docking; hormone recognition.

INTRODUCTION

Insulin is a small (~6 kDa) dual-chain peptide hormone secreted by the pancreatic β cells,[1] which is chiefly responsible for glucose homeostasis in higher organisms. The physiological action of insulin is mediated by the insulin receptor (IR), a close homologue of the type-1 insulin-like growth factor receptor (IGF1R), both of which are constitutively homo-dimeric transmembrane glycoproteins of the receptor tyrosine kinase (RTK) superfamily.[2–5] Each monomer in the receptor homo-dimer is comprised of two leucine-rich domains (L1 and L2) separated by a cysteine-rich (CR) domain and followed by three fibronectin type-III repeats, F1, F2, and F3, which is connected via a single transmembrane helix to the intracellular kinase domain.[6] Although the molecular details of insulin binding and receptor activation remain elusive, partly due to the lack of structure of the hormone-bound receptor, the crystal structure of apo-IR (IRΔβ[7]; PDB code 2DTG) has provided structural bases for domain organization in the IR homodimer,[8–13] where subunits are arranged in a "folded-over inverted V" conformation with each of the two insulin-binding pockets formed by the (L1–CR–L2) motif of one subunit and the (F1–F2–F3) motif of the other subunit. A homology model of the IGF1R ectodomain validated by small-angle X-ray scattering (SAXS) data displays similar overall architecture.[14]

Additional Supporting Information may be found in the online version of this article.

Abbreviations: CT, C-terminal peptide; ID, insert domain; IGF1R, type-1 insulin-like growth factor receptor; IR, insulin receptor; MC, Monte-Carlo; MD, molecular dynamics; TAMD, temperature-accelerated molecular dynamics.

Grant sponsor: National Science Foundation; Grant numbers: DMR-6427643, CBET-0544933 and TG-MCB070073N
*Correspondence to: Harish Vashisth, Department of Chemistry and Biophysics Program, University of Michigan, Ann Arbor, MI. E-mail: harishv@umich.edu
Received 10 September 2012; Revised 11 December 2012; Accepted 4 January 2013
Published online 24 January 2013 in Wiley Online Library (wileyonlinelibrary.com). DOI: 10.1002/prot.24255

Furthermore, site-specific mutagenesis, photo cross-linking, and chimeric receptor studies have provided detailed information on residues involved in the hormone/receptor interfaces.[3–5,8,11,15–38] Specifically, insulin and IR interact via "site-1" and "site-2" epitopes (Supporting Information Table S1): the site-1 residues of IR reside in the central β-sheets of the L1 domain and in a structural motif of the F2 domain known as the C-terminal peptide (CT), while site-2 residues of IR belong to the C-terminal loops of F1 and the N-terminal loops of F2; and the site-1/2 of insulin have residues both from the A- and B-chain. All hormone-binding residues of IR were resolved in the IRΔβ structure (PDB code 2DTG), except for those in CT. Importantly, Smith *et al.*[39] have now unambiguously resolved residues 693–710 of CT along the L1 surface of IR. The refined IRΔβ structure (PDB code 3LOH) shows that the CT-peptide is an α-helix packed against the chiefly nonpolar surface of the central β-sheets of the L1 domain (Supporting Information Fig. S1). Despite nearly-complete characterization of the hormone-binding epitopes of IR, it has proven difficult to reconcile mutagenesis data for following reasons: (a) known crystal structures of the wild-type hormone display an inactive storage form,[40] where a key receptor-binding surface of hormone remains hidden; (b) the exact mechanism of the reorganization of the C-terminus of the B-chain of insulin that exposes the N-terminal residues of the A-chain[41–44] on receptor binding remains unknown; and (c) a model of the hormone/receptor complex[45] would imply significant structural overlap between insulin and CT,[39] suggesting displacement of CT by insulin[10] with additional likely structural rearrangements in the hormone as well as the receptor.

Using the structures of the apo-ectodomains of IR[7] and IGF1R,[14] we have previously proposed all-atom structural models for the ligand/receptor complexes.[46,47] These structural models provide molecular description of many residue-based contacts at the ligand/receptor interfaces, and delineate asymmetric flexibility mechanisms of receptors that are consistent with the notion of a "see-saw" model of negative cooperativity in insulin binding[7,48] and a "harmonic-oscillator" model of receptor activation.[49] Nonetheless, our insulin/IRΔβ structural models[46] remain limited due to: (a) the absence of then-unresolved CT-peptide, a critical structural element[50] without which IR has drastically reduced affinity for insulin,[22,29–32] and (b) the absence of any significant conformational change in the receptor-bound intact T and R insulin needed to explain interaction of several insulin residues with L1.

However, the availability of new structural information on the CT-peptide,[39] and a novel conformational sampling algorithm for proteins[51] provide a timely opportunity to address following yet unresolved key questions: (1) Is it possible to accommodate intact T and R insulin in either of the two binding pockets of IRΔβ with CT present in the same location and conformation as observed in the refined IRΔβ structure?[39] (2) If yes, how thermodynamically costly are conformational changes in insulin that displace the C-terminus of the B-chain under the condition that CT remains in its crystallographic position? We have now addressed these questions by first constructing all-atom structural models of T and R insulin with IRΔβ in the presence of CT, and then characterizing the conformational change in the C-terminus of the B-chain of each insulin using a judicious combination of temperature-accelerated molecular dynamics (TAMD)[51–53] and the string method in collective variables (CVs).[54] Our analyses of these structural models argue for a different mode of insulin binding in which the incoming ligand displaces the potentially flexible helical CT peptide via its canonical B-chain helix. More importantly, this "alternative" mode of insulin binding (where CT is displaced) is thermodynamically favorable and also helps rationalize observations on helical insulin mimetic peptides that can compete with CT for binding to L1,[50] and can serve as high-affinity agonists/antagonists of IR.[55,56]

METHODS

Molecular dynamics simulations and Monte-Carlo docking

All docking calculations were carried out using our previously successful MD-assisted Monte-Carlo (MC) docking algorithm where independent conformational sampling of both ligand and receptor is carried out from solvated and MD-equilibrated solution ensembles of each protein along with MC translational and rotational trial moves (see Supporting Information Methods for additional details).[46,47,57] All MD and TAMD simulation trajectories were generated using NAMDv2.8[58] and the CHARMM force-field[59] with the CMAP correction.[60] VMDv1.9[61] was used for system creation and protein rendering (see Supporting Information Methods for simulation set-up and execution).

RESULTS

T/IRΔβ and R/IRΔβ structural models with CT

Using an MD simulation assisted MC docking algorithm,[46,47,57] we constructed docked structural models of T/IRΔβ and R/IRΔβ complexes in the presence of a crystallographically positioned CT peptide. Briefly, we first incorporated the CT-peptide (from the refined IRΔβ structure; PDB code 3LOH) in apo-IR conformations that allowed binding of intact T and R insulin previously,[46] and performed MC docking using independent conformational sampling of each ligand from an ensemble of solution conformations generated via MD simulations (see Supporting Information Methods for details on complex generation). Two final models (one for each in-

sulin/receptor complex) that display highest degree of agreement with experimentally known insulin/IR interactions are shown in Figure 1. Overall, each intact insulin molecule could be docked relatively easily despite the presence of CT (in the same conformation as observed in refined IRΔβ structure; PDB code 3LOH) in the binding pocket, confirming our earlier speculation.[46] Specifically, these structural models have following salient features at site-1: (i) the side-chain of Val^{B12} sits close to Leu^{36} and Asp^{12} (L1) in T/IRΔβ, while the same side-chain interacts with Leu^{36} and Gln^{34} (L1) in R/IRΔβ; (ii) the side-chain of Tyr^{B16} lies in close proximity to Phe^{39} (L1) and His^{710} (CT) in both complexes; (iii) Glu^{B13} salt-bridges to Arg^{14} (L1) in T/IRΔβ; however, the same residue salt-bridges to Lys^{703} (CT) in R/IRΔβ; (iv) the side-chain of His^{B10} is in the proximity of Lys^{703} and Thr^{704} (CT) in T/IRΔβ, but does not contact any residue of CT in R/IRΔβ; (v) the side-chains of Phe^{B24}, Phe^{B25}, and Tyr^{B26} in both models do not directly contact any residue of L1/CT because the C-terminus of the B-chain (B21–B30; labeled C in Fig. 1) lies in a narrow cleft between the L1 and CR domains; (vi) due to the hindrance posed by the C-terminus of the B-chain of each insulin, no contacts between the A-chain of either insulin with L1/CT are observed. At site-2: (i) in T/IRΔβ, the cluster formed by the side-chains of Ser^{A12}, Leu^{A13}, Tyr^{A14}, and Glu^{A17} interacts with Leu^{552}, Arg^{554}, Lys^{557}, and Leu^{558} (F1), while Leu^{B17} and Val^{B18} interact with Asp^{483} and Lys^{484}; (ii) in R/IRΔβ, the side-chains of Ser^{A12}, Leu^{A13}, Tyr^{A14}, and Glu^{A17} interact with Lys^{484} and Leu^{552}, while Leu^{B17} and Val^{B18} interact with Arg^{554}, Lys^{557}, and Leu^{558} (F1).

Each of these structural models was further equilibrated for 11 ns via explicit-solvent MD simulations (see Supporting Information Results for dynamics of the receptor and bound-ligands during these MD trajectories). Both insulin molecules remain stably bound along with CT on this time-scale. However, neither of the insulin molecules undergoes any significant conformational change in their C-terminus of the B-chain (B21–B30) during MD equilibration, precluding the observation of contacts between the N-terminal residues of the A-chain with L1/CT. Previously,[46] our relatively longer unbiased simulations also failed to show this well-known[41–43,62,63] conformational change in the C-terminus of the B-chain of receptor-bound insulin that mediates specificity of hormone binding to IR,[64] likely because the underlying free-energy barriers are difficult to surmount on reasonable time-scales. To further understand the flexibility of the C-terminus of the B-chain of each insulin, we carried out longer (10 ns) explicit-solvent MD equilibration runs of

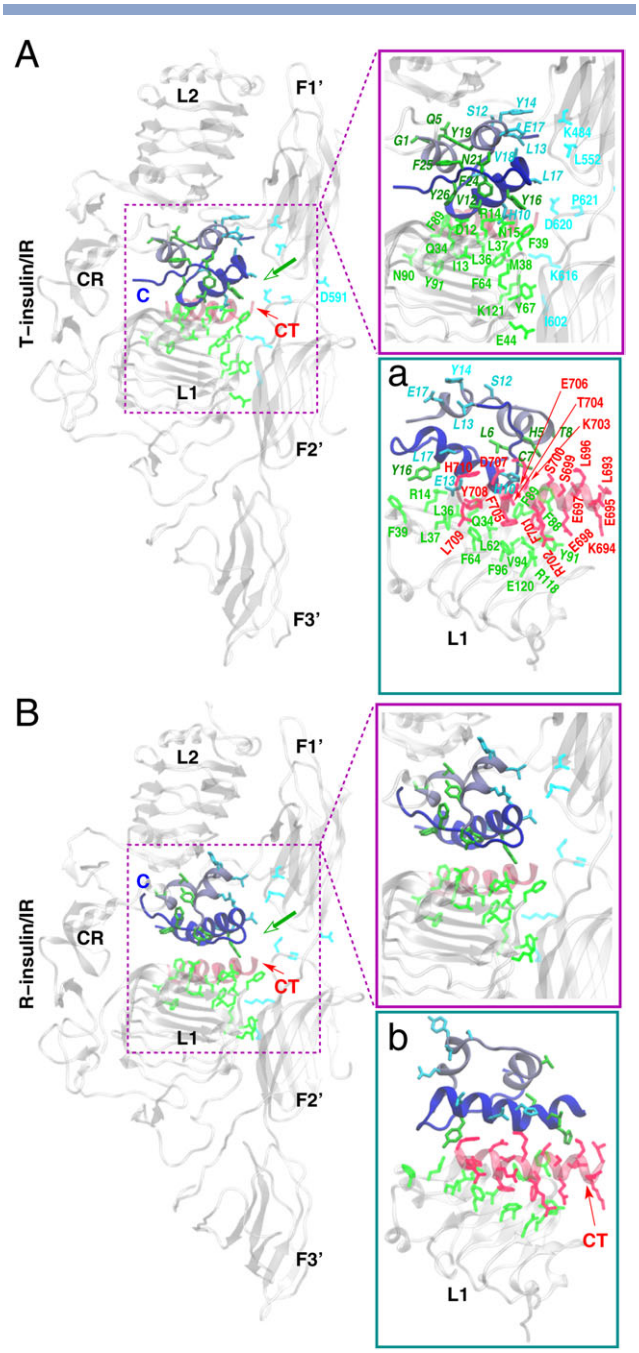

Figure 1

Representations of Monte-Carlo (MC) docked and energy-minimized configurations of (**A**) T-insulin/IRΔβ complex, and (**B**) R-insulin/IRΔβ complex in presence of the CT-peptide. Receptor domains are shown in transparent white cartoons, and the A- and B-chain of each insulin are in the light-blue and dark-blue cartoons, respectively. The C-terminus of the B-chain of each insulin is labeled C, and the C-terminal peptide (CT) of IR is labeled and depicted as red cartoon. Known site-1 and site-2 residues of insulin and IR (zoomed views) are labeled (only for T/IRΔβ complex) and shown in color as sticks: green indicates site 1 residues on insulin and IR, while cyan indicates corresponding site 2 residues for both. The labels for the site-1 and site-2 residues of insulin in each ligand/receptor complex are italicized. Green arrows in the left panels indicate viewing directions for insets *a* and *b* on the right, which highlight residue–residue contacts between each insulin, CT-peptide, and the L1 domain. The snapshots of residue–residue contacts for each insulin/IRΔβ complex after MD equilibration are shown in the Supporting Information. [Color figure can be viewed in the online issue, which is available at wileyonlinelibrary.com.]

wild-type T and R-insulin. From these runs, we observed that R-insulin can spontaneously undergo a conformational change in the C-terminus of its B-chain that exposes the residues in the N-terminus of the A-chain (Supporting Information Fig. S15). We note that our MC trials to dock this "pre-opened" R-insulin with CT in its crystallographic position (PDB code 3LOH) failed to achieve a successful docking likely due to steric clashes between the C-terminus of the B-chain and the domains of IR. Hence, we resorted to a recently proposed conformational sampling algorithm for proteins by Abrams and Vanden-Eijnden[51] based upon the TAMD equations[52,53] to characterize the conformational change in the C-terminus of the B-chain of each receptor-bound insulin in the T/IRΔβ and R/IRΔβ complexes described above.

TAMD simulations of the C-terminus of the B-chain of receptor-bound insulin molecules

We carried out two (one for each complex) ~40-ns long TAMD simulations of hormone-bound receptor complexes in which the CT of the receptor was not displaced relative to the 3LOH structure, where enhanced conformational sampling of the C-terminus of the B-chain of each insulin was allowed. We chose the Cartesian coordinates of centers of mass of spatially contiguous groups of residues as collective variables (CVs). Particularly, the residues in the C-terminus of the B-chain (B23–B30) of each insulin were divided into four subgroups (four groups of two residues each; 12 CVs), and TAMD was applied to these CVs at a fictitious thermal energy of $\tilde{\beta}^{-1} = 6$ kcal/mol (see Supporting Information Methods). We show evolution of the root-mean squared deviation (RMSD) of the C-terminus of the B-chain residues (B21–B30; C_α) of each insulin, and key buried surface areas (BSA) during TAMD simulations in Figure 2(A). Shown in Figure 2(B) are snapshots at various time-points highlighting the C-terminus of the B-chain, the L1/CR domain, CT, and each insulin molecule. Specifically, we observe the following: (i) the opening of the C-terminus of the B-chain of each insulin (as indicated by increasing RMSD; ①) results in significant exposure of respective insulin molecules (see decreasing BSA between the C-terminal residues of the B-chain of each insulin and rest of the insulin molecules; ②); (ii) exposure of the hydrophobic core of R-insulin molecule is commensurate with remarkable (~five times) increase in BSA between the L1 domain and R-insulin (cyan trace; ③), while T-insulin fails to achieve increased registry with the L1 domain (black trace; ③); (iii) during conformational change in the C-terminus of the B-chain of each insulin, CT does not dissociate and maintains on average similar BSA with L1 as observed in the crystal structure (PDB code 3LOH) for each insulin (④); and

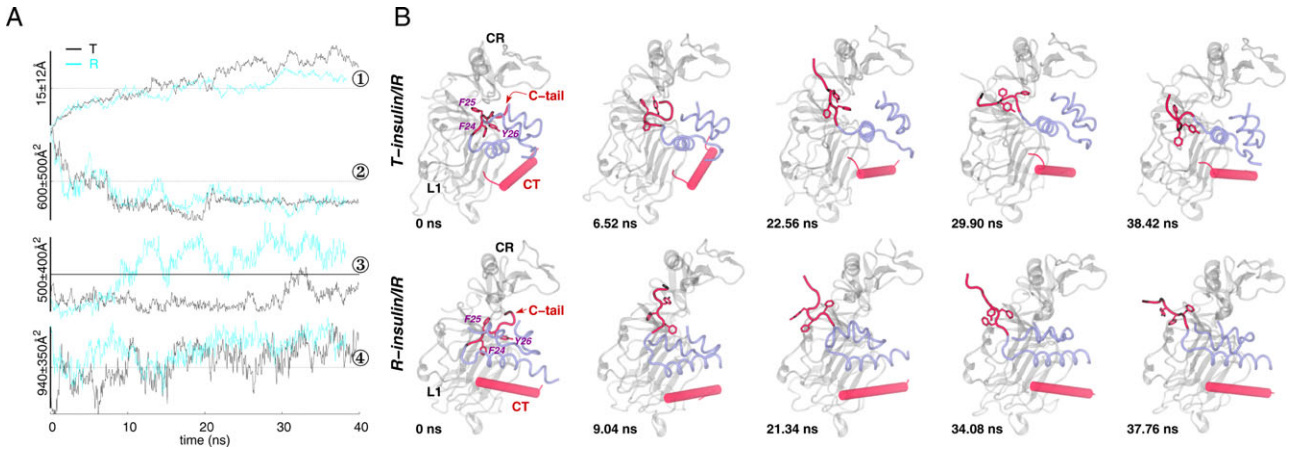

Figure 2

TAMD-generated conformational change in the C-terminus of the B-chain of each insulin. (**A**) Traces (T, black; R, cyan) of the root-mean squared deviation (RMSD) and buried surface area (BSA) versus simulation time (ns) are shown for each insulin/IRΔβ complex. Circled digits indicate the following: (①) RMSD of the C-terminus (residue B21–B30) of the B-chain of each insulin. For RMSD computation, the insulin molecules were aligned based upon the residues of each A- and B-chain (A1–A21 and B1–B20; C_α); (②) BSA between the C-terminus of the B-chain (residues B21–B30) of the B-chain of each insulin and rest of the insulin molecules; (③) BSA between each insulin molecule (except the B-chain residues B21–B30) and the L1 domain; and (④) BSA between CT and the L1 domain. Horizontal lines indicate the values measured in the IRΔβ crystal structure (PDB code 3LOH) except the dotted horizontal lines that are arbitrarily drawn for guidance. (**B**) Conformational change in the C-terminus of the B-chain of each insulin is highlighted. Representative snapshots of each insulin (transparent blue), CT (transparent red), and the L1 and CR domains of IRΔβ (transparent white) are shown at various time-points of respective TAMD simulations. The residues F^{B24}, F^{B25}, and Y^{B26} are shown in sticks and labeled in the first snapshot for each insulin/IRΔβ complex. Initial positions of CT are different (from the crystal structure) for each insulin/IRΔβ complex because TAMD trajectories were started based upon the MC-docked and MD-equilibrated structural models of each insulin/IRΔβ complex (see Supporting Information results for the position of CT during ~11-ns MD-equilibration of each complex). Some of the terminal residues of CT spontaneously fold/unfold during TAMD trajectories. [Color figure can be viewed in the online issue, which is available at wileyonlinelibrary.com.]

(iv) the C-terminus of the B-chain of each insulin moves through a narrow cleft between the L1 and CR domain to the top of L1, where it stably fluctuates for the last 10 ns of each TAMD trajectory. The dynamics of receptor during TAMD simulations is described in Supporting Information Results.

Thermodynamics of conformational change in each insulin via string method

The fact that TAMD[51–53] allows exploration of the physical free-energy surface for conformational sampling implies that conformations observed under TAMD are statistically significant,[65,66] suggesting insulin molecules can undergo structural changes (in the C-terminus of the B-chain) that result in exposure of their hydrophobic core for recognition by IR. However, for a detailed thermodynamic characterization of the transition mechanism, we used the string method in CVs[54,67–71] to refine the pathway generated by TAMD for each insulin toward the minimum free-energy path (MFEP). String method is a technique to compute MFEP in a large but finite set of CVs by iteratively refining an initial "string", that is, a collection of discrete configurations of the system referred to as images (see Supporting Information Methods). Free-energy profiles for the converged pathways appear in Figure 3(A). The profile for T-insulin [black trace; Fig. 3(A)] suggests a significantly high ~37 ± 4.5 kcal/mol free-energy barrier (at image 6) for the transition in the C-terminus of the B-chain of bound-insulin before a metastable intermediate state is observed (at image 8) with $\Delta F \approx 12.67 \pm 9$ kcal/mol (with reference to image 0). The C-terminus of the B-chain in this metastable region, although away from the N-terminal residues of the A-chain, is still located in a narrow cleft between the L1 and CR domains of IR [Fig. 3(B)]. No other metastable intermediate states are observed for T-insulin, and a positive ΔF (with reference to image 0) for all images suggests that it is thermodynamically unfavorable for T-insulin to undergo conformational change in the C-terminus of its B-chain with CT peptide present in its nearly crystallographic position as seen in the crystal structure (PDB code 3LOH).

However, we observe a significantly different trend in the free-energy profile for R-insulin [cyan trace; Fig. 3(A)]. Notably observed are metastable states at images 2, 5, 9, and 15–18, and transition states at images 3, 6, and 11. Thermodynamic preference for conformational change observed in aforementioned images is indicated by a negative ΔF (with reference to image 0) for each of these images. A key structural feature in images from 1 to 9 is the separation of the C-terminus of the B-chain [which is positioned between L1 and CR; Fig. 3(B)] that exposes ~50% of BSA (see Supporting Information Results) between the C-terminus of the B-chain (B21–B30) and rest of R-insulin. The relative free-energy difference between images from 1 to 9 is ~2–4 kcal/mol, suggesting a dynamic equilibrium among these conformations where insulin partially exposes its hidden hydrophobic core. Other than placement of the C-terminus of the B-chain of insulin in the proximity of the top rungs of L1, an important distinguishing feature of the transi-

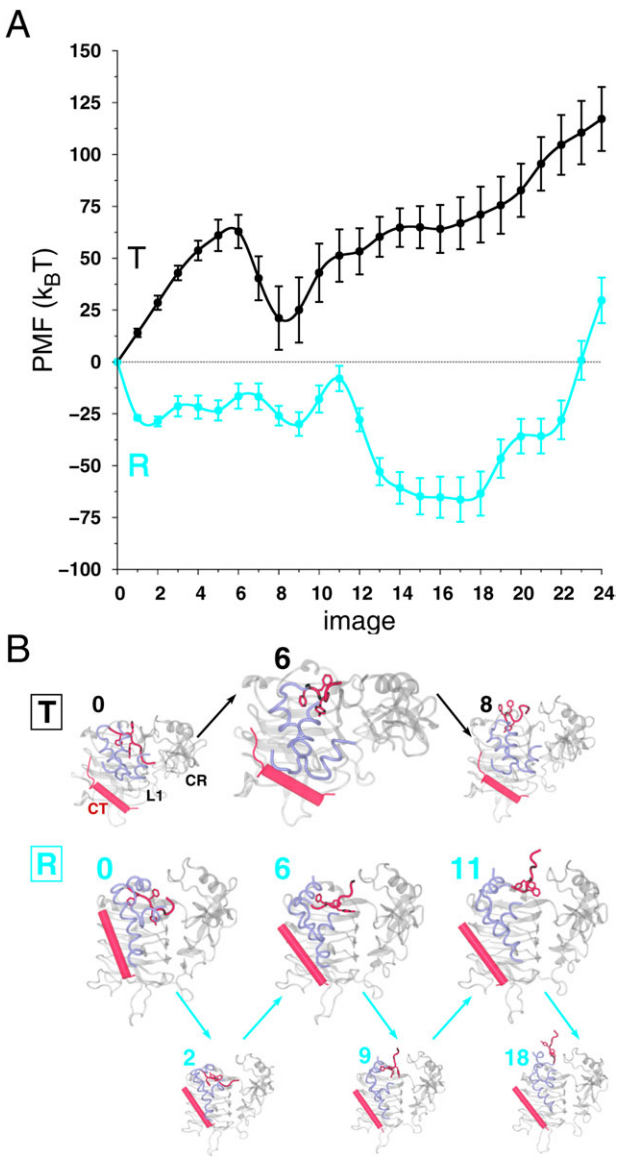

Figure 3

Thermodynamics of conformational change in the C-terminus of the B-chain of each insulin. (**A**) Converged free-energy profiles along the minimum free energy path (MFEP) computed via string method are shown for each insulin. (**B**) Representative snapshots of MFEP images are shown: **T**-insulin (0, 6, and 8); and R-insulin (0, 2, 6, 9, 11, and 18). The larger/smaller panels are higher/lower in free-energy, respectively, and the arrows indicate the same. Compare Figure 2 for coloring and labeling scheme. [Color figure can be viewed in the online issue, which is available at wileyonlinelibrary.com.]

tion state at image 11 is the onset of rotation of insulin molecule (*vide infra*) such that the N-terminal residues of the A-chain directly contact L1, and BSA between R-insulin and L1 significantly increases, consistent with rearrangements spontaneously occurring in TAMD simulation of R-insulin. However, we note that before crossing transition state at image 11, there is a relatively high free-energy barrier of at least ∼15 kcal/mol for conformational change in the C-terminus of the B-chain of R-insulin. Also, further separation of the C-terminus of the B-chain of R-insulin beyond placement on the top of L1 is thermodynamically unfavorable, as indicated by an increase in free-energy at images 19 to 24. The BSA between R-insulin and L1 at initial image 0 and the lowest free-energy image 18 are ∼270 Å^2 and ∼820 Å^2, respectively. The free-energy difference (ΔF) between image 0 and 18 is −39.71 kcal/mol. The CT peptide remains associated with L1 in all MFEP images, and has a BSA with L1 of ∼1120 Å^2 at lowest-free energy image 18.

Highlighted in Figure 4 are the positions of the A- and B-chain of R-insulin on the L1 surface along with CT for MFEP images 0 (red), 12, 18, and 24 (blue). We observe that after reaching the transition state at image 11, the entire R-insulin molecule experiences an anticlockwise rotation (looking at the L1 surface) and also translates toward the top of L1 with its B-chain helix nearly parallel to CT, which places the N-terminal residues of the A-chain (Gly^{A1}, Ile^{A2}, and Val^{A3}) in the vicinity of Asp^{12} and Gln^{34} (L1). After rotation/translation of R-insulin, the side-chain of Tyr^{708} (located near Leu^{36}, Leu^{37}, and Phe^{64} of L1) is the only CT residue closest (∼10 Å) to the A-chain Val^{A3} as highlighted in Figure 4.

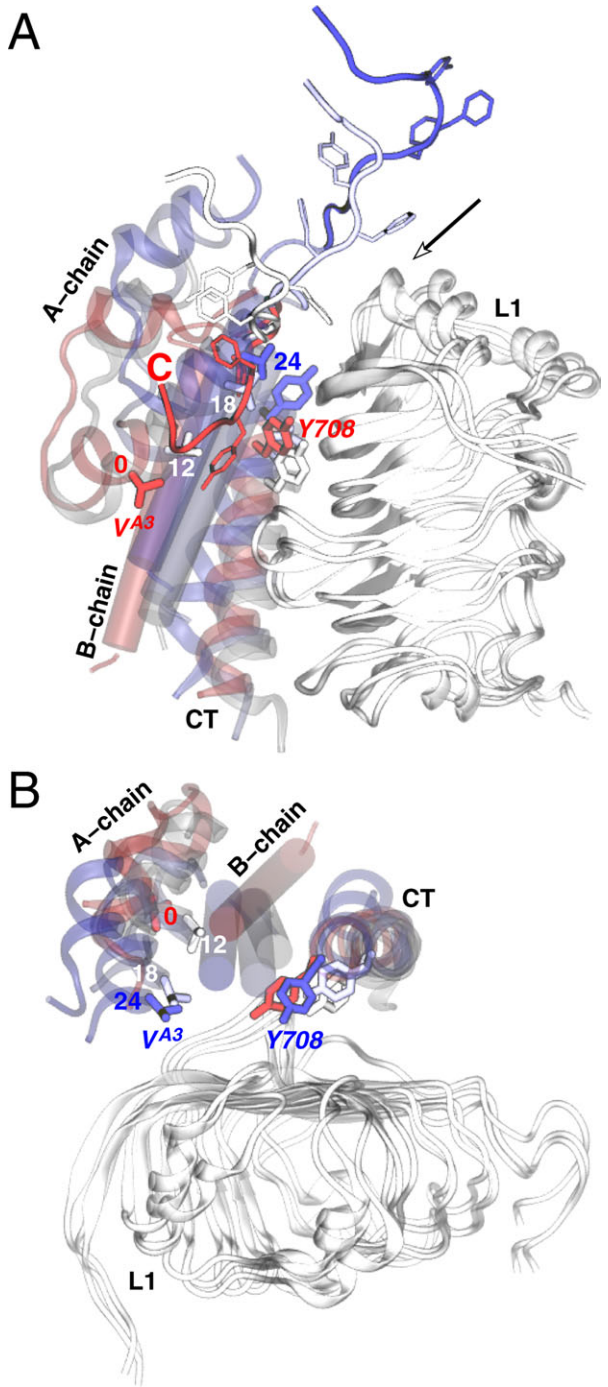

Insulin recognition in a displaced-CT IR

The structural models described above suggest that both T and R-insulin can be docked in one out of two binding pockets of IRΔβ with no major displacement of the CT-peptide. Furthermore, it is thermodynamically unfavorable for T-insulin to undergo conformational change in its flexible C-terminus of the B-chain (B21–B30), while the same conformational change in receptor-bound R-insulin is favorable but the underlying free-energy barriers (required for R-insulin to achieve a tighter registry with L1) are relatively high. Because no contacts between the C-terminal residues of the B-chain (B21–B30) of either insulin and the CT-peptide are observed even after this conformational change, it remains unclear from these structural models how photo-probes in the N-terminal residues of the A-chain of insulin and also in the C-terminal residues of the B-

Figure 4

Orientation of the A-chain of R-insulin. (**A**) Representative snapshots of R-insulin, CT, and the L1 domain from MFEP images 0 (red), 12, 18, and 24 (blue) are shown and labeled. Varying orientation of the A-chain of R-insulin can be traced via the highlighted side-chain of V^{A3}, which is shown in sticks and labeled for image 0 with image index indicating further positions. Shown in sticks and labeled is also the side-chain of Y^{708} (CT). Highlighted also are the positions of the C-terminus of the B-chain of insulin (labeled C in red for image 0) along with the stick representations of F^{B24}, F^{B25}, and Y^{B26}. The black arrow indicates viewing direction for panel (**B**), where similar structural features as in panel (A) are shown except the C-terminus of the B-chain of insulin, which is omitted for clarity. Change in the orientation of the B-chain of insulin and CT are apparent in this view due to conformational change in the insulin-tail (B21–B30). [Color figure can be viewed in the online issue, which is available at wileyonlinelibrary.com.]

chain can crosslink to the CT peptide simultaneously.[39,72] These structurally unexplained observations along with the following additional experimental evidence suggest that the CT peptide is potentially mobile and may be displaced from its crystallographic position by the incoming insulin molecule[10]: (a) site-1 insulin mimetic peptides can compete with CT for binding to the L1 domain of IR,[50] (b) tighter binding of aromatic-substituted CT peptides to apo-IR leads to a commensurate loss of insulin affinity,[39] and (c) the photo-probes in the β-strands 2 and 3 of L1 can efficiently crosslink to insulin despite the fact that they are shielded by CT in the crystal structure (PDB code 3LOH).[73] Interestingly, there is a close structural relationship between the B-chain of R-insulin (B1–B18) and the resolved structure of the CT peptide (693–710): both are 18-residue-long α-helices. Hence, it has been speculated that the B-chain helix of insulin can potentially displace CT peptide.[10] We therefore conjectured that preopened R-insulin (Supporting Information Fig. S15) could dock if CT is displaced. With the above observations in mind, we constructed a second physically plausible structural model of the R-insulin/IRΔβ complex based upon the structural models described above. In this new model, the B-chain helix of R-insulin is presumed to have displaced the CT peptide from its original position, which we mimic by swapping the positions of R-insulin and CT in the lowest free-energy image 18 of the non-CT-displaced minimum free energy path (Fig. 3) based upon the structural alignment of their respective α-helices. This provides a basis for an initial placement of CT different from that in the 3LOH structure and onto which we can repeat MC docking of R-state insulin. We launched MC dockings of the swapped insulin/CT configurations by carrying out independent exhaustive conformational sampling of preopened R-insulin (Supporting Information Fig. S15) and receptor conformations from MD trajectories (see Supporting Information Methods for details). We

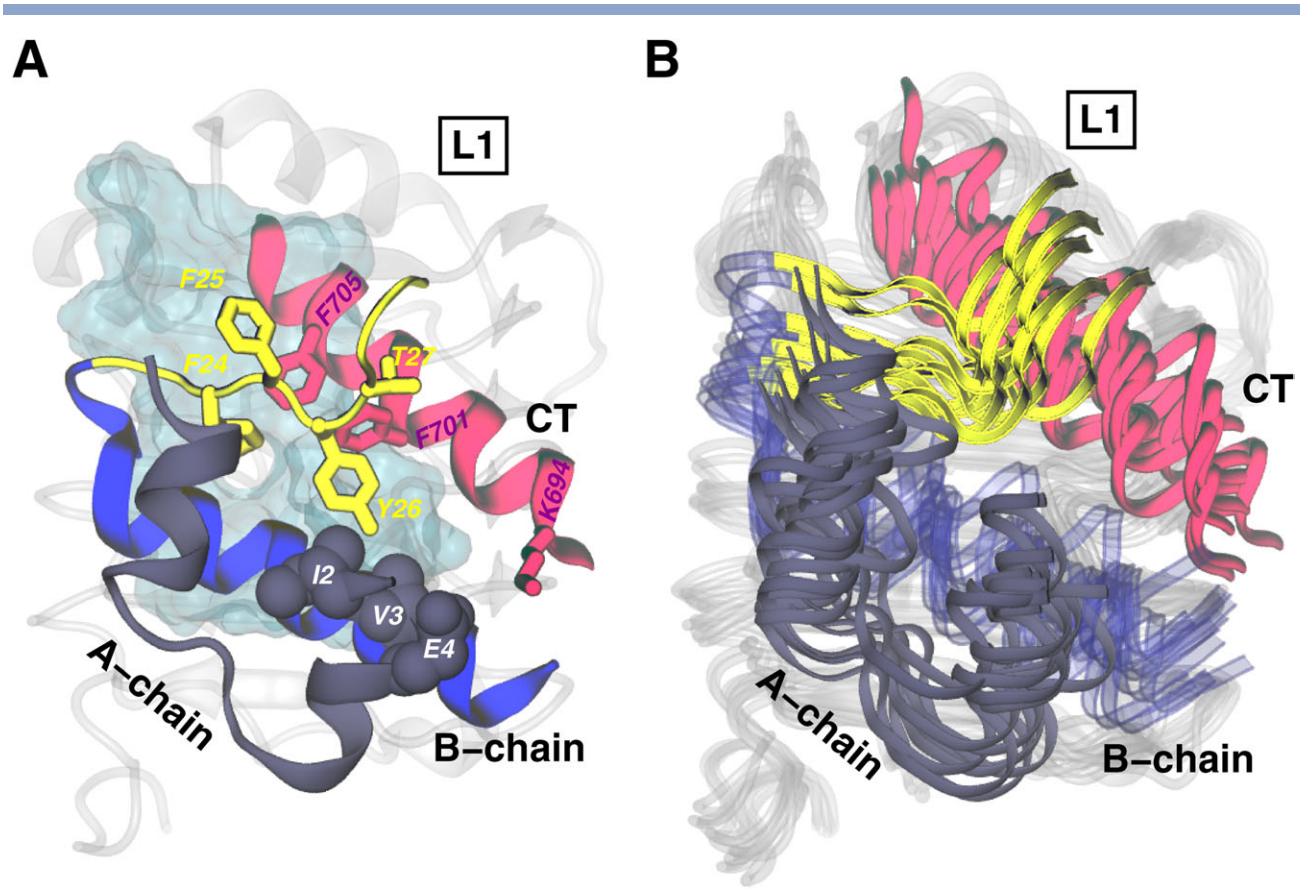

Figure 5

Displaced-CT model of insulin binding. (**A**) Overlay of R-insulin and the CT peptide on the surface of the L1 domain is shown from a typical docking with CT displaced from its original position by the B-chain helix (B1–B19) of insulin. Individual chains of insulin, CT, and L1 are colored and labeled. The flexible C-terminus of the B-chain of insulin is highlighted in yellow along with the sidechains of key residues where PheB24 and TyrB26 are known to crosslink to L1, while PheB25 and ThrB27 are known to crosslink to CT. Colored and highlighted in spheres are the sidechains of the N-terminal residues of the A-chain of insulin IleA2, ValA3, and GluA4 that are known to crosslink to CT. Also shown in sticks are the sidechains of Lys694, Phe701, and Phe705 of CT as reference. Key ligand-binding residues on L1 are also shown as a cyan transparent surface. Other domains of the receptor are omitted for clarity. (**B**) Ensemble of 10 MC-docked configurations of R-insulin and CT on the surface of the L1 domain is shown.

find that both R-insulin and CT can be docked relatively easily without any structural overlap with receptor domains in this displaced-CT model.

We show the overlay of R-insulin and CT on the surface of the L1 domain of IR from a typical docked configuration in Figure 5(A), and the conformational variability of R-insulin and CT is depicted by 10 MC-docked configurations shown in Figure 5(B). Looking at the L1 surface [Fig. 5(A)], CT has now been displaced to the right of insulin in comparison to its original crystal structure position which is approximately occupied by the B-chain helix of R-insulin. Furthermore, both ligand and CT are still located in proximity to the ligand-binding patch on L1 [transparent cyan surface in Fig. 5(A)] where they can achieve specific registry with L1. Most importantly, this model helps rationalize photo-crosslinking experiments[72] which suggest that the N-terminal residues of the A-chain of insulin (IleA2, ValA3, and GluA3) directly crosslink to CT, which is possible in our newer model given their proximity to the N-terminus of CT [Fig. 5(A)]. The bifunctional derivatives of photoprobes have further indicated that PheB24 and PheB26 crosslink to L1, while surprisingly, probes at residues PheB25 and ThrB27 crosslink to CT.[39] This is possible in the displaced-CT model as the sidechains of B24/B26 are oriented toward L1, and of B25/B27 are oriented toward the C-terminal end of resolved CT. We note that such placement of the flexible C-terminus of the B-chain of insulin (yellow cartoon in Fig. 5) has been possible due to a spontaneous separation of the C-terminus of the B-chain of ligand from the rest of R-insulin in a longer unbiased MD simulation (Supporting Information Fig. S15). As mentioned above, it is interesting to point out that the conformations of R-insulin, where the C-terminus of the B-chain is detached from rest of the insulin molecule, fail to dock in the receptor with CT in nearly crystallographic position. The orientation of R-insulin in this displaced-CT model also places the site-2 surface of ligand in the proximity of the (F1–F2)′ loops where site-2 residues on receptor are located (Supporting Information Fig. S16). Equilibration of this R-insulin/IRΔβ complex is described in Supporting Information Results and Supporting Information Fig. S17.

The facts that it was relatively easy to dock R-insulin/CT in the swapped states, and the entire complex remains intact during MD-equilibration, suggest that the B-chain helix of R-insulin can potentially displace CT from its crystallographic position. However, it is not yet clear if such placement is also thermodynamically favorable, which we further tested. To understand the relative free-energy differences between microscopically distinct MC-docked conformations in the displaced-CT model, we further carried out string method calculations (see Supporting Information Methods) by evolving toward MFEP an initial string comprised of 10 MC-docked configurations. Because docked R-insulin had already undergone conformational change in the C-terminus of its B-chain, as collective variables to compute the free-energy profiles via the string method, we used the center-of-mass coordinates of R-insulin and CT to allow their better placement on the L1 surface. We show the free-energy profile from the converged string as well as from each string-

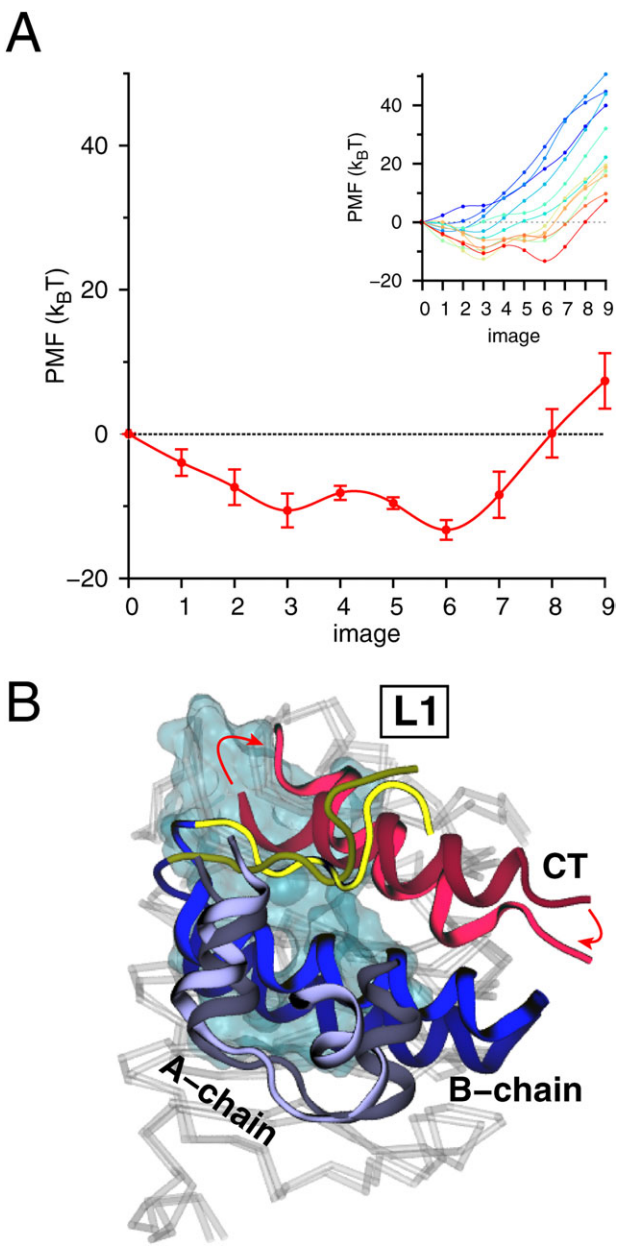

Figure 6

Thermodynamics of MC-docked configurations of the displaced-CT model. (**A**) Converged free-energy profile (red trace) along the minimum free energy path (MFEP) computed via string method is shown for the R/IRΔβ complexes in the displaced-CT model. Inset shows the free-energy profiles at each string iteration (blue; first iteration, and red; last iteration). (**B**) Overlay of R-insulin and CT on the surface of the L1 domain of IR is shown for metastable MFEP images 3 (dark color cartoons) and 6 (light color cartoons). Arrows depict the clockwise rotation of CT during transition from image 3 to image 6. Compare Figure 5 for coloring and labeling scheme. [Color figure can be viewed in the online issue, which is available at wileyonlinelibrary.com.]

iteration in Figure 6(A). The converged free-energy profile [red trace in Fig. 6(A)] shows that the majority of MC-docked configurations have a negative ΔF (with reference to image 0), suggesting that it is thermodynamically favorable to place R-insulin and CT in swapped configurations. The free-energy profile further reveals two metastable intermediates among 10 MC-docked models, which belong to images 3 and image 6 with $\Delta F \approx -6.33 \pm 1.40$ kcal/mol and -7.95 ± 0.82 kcal/mol, respectively. A small free-energy barrier of $\sim$1.5 kcal/mol (image 4; transition state) is observed between images 3 and 6. We observe two key structural differences in R-insulin/CT configurations at images 3 and 6 [Fig. 6(B)]: both R-insulin and CT rotate clockwise from image 3 to image 6, resulting in lowering of the free energy and better positioning of R-insulin/CT on the L1 surface. These data jointly suggest that the displacement of CT by the R-insulin is thermodynamically favorable, and the underlying free-energy barriers for the adjustment of R-insulin and CT on the L1 surface are relatively low.

DISCUSSION

In this work, we have endeavored to understand the conformational reorganization of insulin on binding to its receptor in the presence of a recently resolved[39] critical tandem hormone-binding element, the CT-peptide. Our previously successful MD-assisted MC docking algorithm[46,47,57] demonstrates that both T- and R-insulin can be accommodated along with the crystallographically positioned CT peptide in one out of two binding pockets of IRΔβ without any major displacement of CT. Specifically, the contacts of Tyr^{B16} with Phe^{39} (L1) for each insulin are consistent with previous models[45,46] and photo crosslinking studies.[74] A key B-chain residue of insulin is Val^{B12}, that has been suggested to contact L1,[74] as observed here: Val^{B12} contacts Leu^{36} and Asp^{12} (L1) in T/IRΔβ complex, and Leu^{36} and Gln^{34} (L1) in R/IRΔβ complex. The side-chain of Glu^{B13}, the mutations of which disrupt insulin binding to IR,[17,75] salt-bridges to either Arg^{14} (L1) in T/IRΔβ or Lys^{703} (CT) in R/IRΔβ. Both models suggest a Glu^{B13} site-1 contact with IR, as opposed to site-2 contact with IR.[4,5] The side-chain of His^{B10} partially interacts with Lys^{703} and Thr^{704} (CT) in T/IRΔβ, and does not contact any IR residue in R/IRΔβ, leaving open the possibility of it being a site-2 contact with IR.[4,5] The cluster of site-2 residues of each insulin (Supporting Information Table S1) Ser^{A12}, Leu^{A13}, Tyr^{A14}, Glu^{A17}, Leu^{B17}, and Val^{B18} interacts (see Results) with suggested[33] site-2 residues in the fibronectin loops of IR (Asp^{483}, Lys^{484}, Leu^{552}, Arg^{554}, Lys^{557}, and Leu^{558}). The observation that each insulin can contact site-1 residues in the L1 domain of one subunit and site-2 residues in the fibronectin domain (F1) of the other subunit of IR is of particular significance, because it suggests crosslinking of receptor subunits by insulin which was demonstrated earlier.[76]

Furthermore, our characterization of the conformational change in the C-terminus of the B-chain of T- and R-insulin via TAMD simulations and the string method suggests that: (i) each insulin molecule can undergo conformational change in the C-terminus of the B-chain (B21–B30), but such opening of the C-terminus of the B-chain in receptor-bound ligands is thermodynamically favorable only for R-insulin albeit involving high free-energy barriers; (ii) this conformational change exposes the hydrophobic core of each insulin, but the exposed surface of only R-insulin achieves significantly increased registry with the L1 domain due to the rotation/translation of R-insulin molecule (Fig. 4). Registry with L1 for T-insulin is largely prevented due to steric hindrance posed by the unfolded conformation of the N-terminus of the B-chain (B1–B8); (iii) the side-chain of Thr^{A8} does not directly contact any IR residue, consistent with suggestions that hormone–receptor interface is not tightly packed at this site because diverse A8 substitutions are easily tolerated.[77]

These structural models where CT is not significantly displaced from its crystallographic position, however, fail to explain some key photo-crosslinking and mutational experiments[21,30,39,72,73,78] as well as the observations from helical insulin mimetic peptides[50,55,56], which suggest that CT is potentially mobile and needs to be displaced by insulin[10] for it to achieve specificity with the L1 domain of IR. Considering these aspects, we constructed a second R-insulin/IRΔβ structural model based upon the observation that the positions of the B-chain helix of only R-insulin (B1–B18) and α-helical CT (693–710) can be easily swapped without any structural overlap with any receptor domain, and also that R-insulin can spontaneously undergo conformational change in its C-terminus of the B-chain (B21–B20) on a longer MD equilibration (Supporting Information Fig. S15). The displaced-CT model suggests that it is now possible for photo-probes in the N-terminal residues of the A-chain of insulin to crosslink to residues in the N-terminus of CT, while probes in the C-terminus of the B-chain at B24/B26 can crosslink to L1 and B25/B27 can crosslink to CT, as suggested before.[29,39,72] The most direct experimental evidence in favor of the displacement of CT by insulin (as suggested by our model) comes from recent photo-crosslinking experiments of Whittaker *et al.*[73] (See, however, the Note in Proof.) These experiments showed that the side-chains of L1 residues Leu36, Leu37, Leu62, and Phe64, normally buried in the αCT/L1 interface of IRΔβ,[39] can efficiently and predominantly crosslink to the B-chain of insulin, which means that CT needs to be displaced for insulin to contact these side-chains. Also, the orientation of R-insulin in our model is consistent with ligand crosslinking of receptor subunits[76] because the ligand can maintain simultaneous contact at site-1 with L1 and at site-2 with the $(F1–F2)'$ loops. These observations are also in accord with a pro-

posed sequential model of association of insulin-binding sites 1 and 2 to IR.[79] As a next step, this new structural model also helps explain recognition of IR by homologous (to insulin) noncognate ligands such as a single-chain polypeptide insulin-like growth factor-1 (IGF1), which cannot undergo significant separation of its C-domain due to single-chain structural constraints. Specifically, we show in Supporting Information Fig. S18 an overlay of IGF1 along with insulin and CT on the surface of the L1 domain of IR, where IGF1 A/B-domains are in the same orientation as insulin, and the FYF (23–25) sequence in the C-domain of IGF1 can substitute for the critical FFY (B24–B26) sequence of insulin (see highlighted sidechains of these residues in Supporting Information Fig. S18). We speculate that the position of CT as observed in the crystal structure of apo-IRΔβ (PDB code 3LOH), where CT shields insulin-binding patch on L1 can be a mechanism to protect the ligand-binding surface of the receptor, which can only be exposed by specific binding of insulin or its mimetic via displacement of CT.

An outstanding question in understanding insulin recognition by IR has been the unknown receptor-bound state of hormone, because classical crystallographic conformers of hormone (T and R; the difference is that B1–B8 residues are in an extended conformation in T, while same residues are helical in R) have the receptor-binding surface hidden in their interior.[40] The R-state, however, has been suggested to be less stable, but more active (in comparison to more stable, but less active T) form of hormone that binds to IR.[9,45,62,80] Furthermore, extensive experimental investigations of insulin structure[40–44,63,64,72,77,81–95] have proposed a "detachment model", which posits that the C-terminus of the B-chain (B21–B30) of insulin detaches itself (from rest of the insulin molecule) via an "induced-fit" mechanism such that the residues in the N-terminus of its A-chain are exposed. The proposed induced-fit in the C-terminus of the B-chain (B21–B30) also lends support to photo-crosslinking studies suggesting that probes at A1–A4, A8, A14, B25, and B27 crosslink to the same CT-peptide, while probes at B16, B24, and B26 crosslink to the L1 domain.[29,39,63,72,74,78] Using TAMD simulations and string method calculations, we find that the receptor-bound T-insulin cannot undergo this conformational change via a thermodynamically favorable path, while the receptor-bound R-insulin can undergo this change to a certain extent beyond which it needs to overcome relatively high free-energy barriers. Interestingly, we also observe via unbiased simulations that free wild-type R-insulin can spontaneously separate the C-terminus of its B-chain (Supporting Information Fig. S15) to expose the residues in the N-terminus of the A-chain. Given that we can readily dock this exposed conformation of R-insulin along with CT in our displaced-CT model suggests that the opening of the B-chain C-terminus alone may not be the basis of the induced fit, but that insulin recognition by IR may be merely a ligand conformational-selection phenomenon. However, it is not unlikely that further conformational changes in R-insulin on binding to receptor might be required to achieve high-affinity recognition. Observation of a spontaneous conformational change in R-insulin and a thermodynamically favorable displacement of CT by the B-chain helix of R-insulin (B1–B19) in our displaced-CT model suggest that R-insulin may be the receptor-bound form of hormone, in accord with earlier experiments.

Finally, we speculate on the implications of this work on the negative-cooperativity of high-affinity insulin-IR binding.[16,48,96] The CT-peptide lies at the C-terminus of the so-called insert domain (ID), an excursion from the second folded type-III fibronectin (F2) domain. At least one disulfide bridge in the Cys-triplet (682, 683, and 685) links the two IDs[97], presumably beneath the apex of the folded-over arch of the dimeric receptor. If one CT is displaced as we suggest here, the connectivity to the other CT through the ID disulfide might hinder the displacement of the CT of the other monomer, making it much more difficult to realize a high-affinity bound state on both sides of the receptor. Consistent with these ideas, we point out that many receptor constructs have indeed been experimentally studied that suggest the role of one or more intersubunit disulfides in high-affinity insulin binding and negative cooperativity. Particularly, the dimeric receptor constructs that contain either a disulfide at Cys524 or a disulfide at the Cys-triplet alone fail to show high-affinity binding and negative cooperativity.[3,97,98] Interestingly, however, both high-affinity binding and negative cooperativity could be restored in dimeric receptor constructs where disulfides at Cys524 and at least one of Cys682/Cys683/Cys685 are simultaneously present.[26] Therefore, it appears that the role of at least one disulfide at Cys-triplet (682, 683, and 685) is to provide a structural constraint that can allow high-affinity insulin binding only in one out of two ligand-binding pockets of IR. Based upon our distance measures between the membrane-proximal domains of IR in apo and ligand-bound simulations (see Supporting Information Discussion, and Supporting Information Table S2), we speculate that constraints on receptor legs via membrane anchors may further help insulin in achieving high-affinity and specificity for IR.[99–101]

Limitations of all-atom structural models

We note that structural models presented here are biased toward the crystallographic conformation of IRΔβ,[7,39] which has missing residues (IDα, 656–719; IDβ 724–754). We point out that the orientation of R-insulin and CT on the L1 surface in the displaced-CT model represents a metastable state and further rearrangements in insulin/CT may still occur for both to achieve specificity with L1. (See again the Note in Proof.)

The exact position of CT on L1 is likely also governed by the structural constraints posed by the missing linkers. Therefore, we point out that the novel physically-plausible placement of CT in our displaced-CT model remains a testable prediction for future experiments. We also point out that several experimental studies have previously estimated binding affinity of insulin for various receptor constructs.[26,27,31,32,100,101] Although the potential of mean force (PMF) calculation should be able to provide an estimate of binding affinity of insulin in principle, we have expressly chosen not to make comparisons to known experimental estimates of binding affinity for the following reasons: (1) The first PMFs that we have computed (Fig. 3) here are for the conformational reorganization of insulin on receptor binding. Specifically, the free-energy difference is associated with the conformational change in the C-terminus of the B-chain of insulin, which possibly contributes to an unknown extent to the binding-affinity of insulin. The second PMF calculation (Fig. 6) provides free-energy differences between different MC-generated states of preopened insulin/CT. Therefore, these free-energy differences are related to both the placement of preopened insulin as well as the displacement of CT, and are likely not separable into individual contributions; and (2) The receptor structure we have used here to construct our structural models has missing structural elements in the insert domains, both downstream and upstream of CT. We have not attempted to model these large unstructured missing portions of IR without any experimental data to guide their placement. These missing structural elements may also contribute to binding affinity, and hence a direct and fair comparison may not be feasible at this point. However, if one were to assume that there is no net free-energy change associated with the movement of CT on the L1 surface, the free-energy change (ΔF) we have reported for our displaced-CT model is ≈ -7.0 to -8.0 kcal/mol, which corresponds to a sub-nanomolar (nM) affinity for insulin in our structural models. This is in qualitative agreement with known nanomolar (nM) affinity of insulin for soluble receptors in the presence of CT. Also, we have not explored the role of membrane-anchors, and neither have we attempted to understand the role of glycosylation, which remain ambitious goals for future studies.

CONCLUSIONS

In this work, we have attempted to understand the interplay of conformational changes involved in binding of insulin to IR in the presence of a potentially flexible tandem hormone-binding element, the CT peptide. With the help of MC docking, MD simulations, TAMD simulations, and the free-energy calculations via string method, we propose potential modes of insulin recognition by IR, which are consistent with a plethora of experimental evidence, and help rationalize some yet unexplained photo-crosslinking studies. Our models support the experimental view that the B-chain helix of R-insulin (B1–B19) can potentially displace flexible CT for insulin to achieve specificity with the L1 domain of IR. We also offer details that suggest R-insulin as a candidate for specific recognition by IR as previously suggested by others based on various experiments.[9,45,62,80]

NOTE ADDED IN PROOF

A crystallographic structure of insulin bound to CT-containing minimal receptor constructs appeared in print after acceptance of our article [Menting et al., Nature 2013 493:241–245]. We briefly mention that, although the detailed registry of residue contacts between insulin and IR in our model do not match this new structure, displacement of CT from its position in the 3LOH structure is confirmed. We also point out that the minimal receptor constructs lack many receptor domains, and when aligned into a full ectodomain structure, the new insulin-bound structure suffers many severe steric clashes with these domains. We are currently working to resolve the disagreement and clashes using our docking methods and will report on them in a future publication.

REFERENCES

1. Steiner DF. Adventures with insulin in the Islets of Langerhans. J Biol Chem 2011;286:17399–17421.
2. Kitamura T, Kahn CR, Accili D. Insulin receptor knockout mice. Annu Rev Physiol 2003;65:313–332.
3. De Meyts P, Whittaker J. Structural biology of insulin and IGF1 receptors: implications for drug design. Nat Rev Drug Discov 2002;1:769–783.
4. De Meyts P. Insulin and its receptor: structure, function and evolution. BioEssays 2004;26:1351–1362.
5. De Meyts P. The insulin receptor: a prototype for dimeric, allosteric membrane receptors? Trends Biochem Sci 2008;33:376–384.
6. Ullrich A, Bell JR, Chen EY, Herrera R, Petruzzelli LM, Dull TJ, Gray A, Coussens L, Liao YC, Tsubokawa M, Mason A, Seeburg PH, Grunfeld C, Rosen OM, Ramachandran J. Human insulin receptor and its relationship to the tyrosine kinase family of oncogenes. Nature 1985;313:756–761.
7. McKern NM, Lawrence MC, Streltsov VA, Lou M, Adams TE, Lovrecz GO, Elleman TC, Richards KM, Bentley JD, Pilling PA, Hoyne PA, Cartledge KA, Pham TM, Lewis JL, Sankovich SE, Stoichevska V, Silva ED, Robinson CP, Frenkel MJ, Sparrow LG, Fernley RT, Epa VC, Ward CW. Structure of the insulin receptor ectodomain reveals a folded-over conformation. Nature 2006;443:218–221.
8. Ward CW, Lawrence MC, Streltsov VA, Adams TE, McKern NM. The insulin and EGF receptor structures: new insights into ligand-induced receptor activation. Trends Biochem Sci 2007;32:129–137.
9. Ward C, Lawrence M, Streltsov V, Garrett T, McKern N, Lou MZ, Lovrecz G, Adams T. Structural insights into ligand-induced activation of the insulin receptor. Acta Physiol 2008;192:3–9.
10. Ward CW, Lawrence MC. Ligand-induced activation of the insulin receptor: a multi-step process involving structural changes in both the ligand and the receptor. BioEssays 2009;31:422–434.

11. Lawrence MC, McKern NM, Ward CW. Insulin receptor structure and its implications for the IGF-1 receptor. Curr Opin Struct Biol 2007;17:699–705.
12. Ward CW, Lawrence MC. Landmarks in insulin research. Front Endocrinol 2011;2:76.
13. Ward CW, Lawrence MC. Similar but different: ligand-induced activation of the insulin and epidermal growth factor receptor families. Curr Opin Struct Biol 2012;22:1–7.
14. Whitten AE, Smith BJ, Menting JG, Margetts MB, McKern NM, Lovrecz GO, Adams TE, Richards K, Bentley JD, Trewhella J, Ward CW, Lawrence MC. Solution structure of ectodomains of the insulin receptor family: the ectodomain of the Type 1 insulin-like growth factor receptor displays asymmetry of ligand binding accompanied by limited conformational change. J Mol Biol 2009;394:878–892.
15. Pullen RA, Lindsay DG, Wood SP, Tickle IJ, Blundell TL, Wollmer A, Krail G, Brandenburg D, Zahn H, Gliemann J, Gammeltoft S. Receptor-binding region of insulin. Nature 1976;259:369–373.
16. De Meyts P, Obberghen EV, Roth J, Wollmer A, Brandenburg D. Mapping of the residues responsible for the negative cooperativity of the receptor-binding region of insulin. Nature 1978;273:504–509.
17. Kristensen C, Kjeldsen T, Wiberg FC, Schäffer L, Hach M, Havelund S, Bass J, Steiner DF, Andersen AS. Alanine scanning mutagenesis of insulin. J Biol Chem 1997;272:12978–12983.
18. Chen H, Shi M, Guo ZY, Tang YH, Qiao ZS, Liang ZH, Feng YM. Four new monomeric insulins obtained by alanine scanning the dimer-forming surface of the insulin molecule. Protein Eng 2000;13:779–782.
19. Nakamura T, Takahashi H, Takahashi M, Shimba N, Suzuki E, Shimada I. Direct determination of the insulin-insulin receptor interface using transferred cross-saturation experiments. J Med Chem 2010;53:1917–1922.
20. Williams PF, Mynarcik DC, Yu GW, Whittaker J. Mapping of an NH_2-terminal ligand binding site of the insulin receptor by alanine scanning mutagenesis. J Biol Chem 1995;270:3012–3016.
21. Whittaker J, Whittaker L. Characterization of the functional insulin binding epitopes of the full-length insulin receptor. J Biol Chem 2005;280:20932–20936.
22. Mynarcik DC, Williams PF, Schaffer L, Yu GQ, Whittaker J. Analog binding properties of insulin receptor mutants. J Biol Chem 1997;272:2077–2081.
23. Schaefer EM, Siddle K, Ellis L. Deletion analysis of the human insulin receptor ectodomain reveals independently folded soluble subdomains and insulin binding by a monomeric α-subunit. J Biol Chem 1990;265:13248–13253.
24. Kristensen C, Andersen AS, Hach M, Wiberg FC, Schäffer L, Kjeldsen T. A single-chain insulin-like growth factor I/insulin hybrid binds with high affinity to the insulin receptor. Biochem J 1995;305:981–986.
25. Schlein M, Havelund S, Kristensen C, Dunn MF, Kaarsholm NC. Ligand-induced conformational change in the minimized insulin receptor. J Mol Biol 2000;303:161–169.
26. Brandt J, Andersen AS, Kristensen C. Dimeric fragment of the insulin receptor α-subunit binds insulin with full holoreceptor affinity. J Biol Chem 2001;276:12378–12384.
27. Surinya KH, Molina L, Soos MA, Brandt J, Kristensen C, Siddle K. Role of insulin receptor dimerization domains in ligand binding, cooperativity, and modulation by anti-receptor antibodies. J Biol Chem 2002;277:16718–16725.
28. Kristensen C, Andersen AS, Østergaard S, Hansen PH, Brandt J. Functional reconstitution of insulin receptor binding site from non-binding receptor fragments. J Biol Chem 2002;277:18340–18345.
29. Kurose T, Pashmforoush M, Yoshimasa Y, Carroll R, Schwartz GP, Burke GT, Katsoyannis PG, Steiner DF. Cross-linking of a B25 Azidophenylalanine insulin derivative to the carboxyl-terminal regions of the α-subunit of the insulin receptor. J Biol Chem 1994;269: 29190–29197.
30. Mynarcik DC, Yu GQ, Whittaker J. Alanine-scanning mutagenesis of a C-terminal ligand binding domain in the insulin receptor α subunit. J Biol Chem 1996;271:2439–2442.
31. Kristensen C, Wiberg FC, Andersen AS. Specificity of insulin and insulin-like growth factor I receptors investigated using chimeric mini-receptors. J Biol Chem 1999;274:37351–37356.
32. Molina L, Marino-Buslje C, Quinn DR, Siddle K. Structural domains of the insulin receptor and IGF receptor required for dimerization and ligand binding. FEBS Lett 2000;467:226–230.
33. Whittaker L, Hao C, Fu W, Whittaker J. High-affinity insulin binding: insulin interacts with two receptor ligand binding sites. Biochemistry 2008;47:12900–12909.
34. Zhang B, Roth RA. A region of the insulin receptor important for ligand binding (residues 450–601) is recognized by patients' autoimmune antibodies and inhibitory monoclonal antibodies. Proc Natl Acad Sci USA 1991;88:9858–9862.
35. Fabry M, Schaefer E, Ellis L, Kojro E, Fahrenholz F, Brandenburg D. Detection of a new hormone contact site within the insulin receptor ectodomain by the use of a novel photoreactive insulin. J Biol Chem 1992;267:8950–8956.
36. Schumacher R, Soos MA, Schlessinger J, Brandenburg D, Siddle K, Ullrich A. Signaling-competent receptor chimeras allow mapping of major insulin receptor binding domain determinants. J Biol Chem 1993;268:1087–1094.
37. Hao C, Whittaker L, Whittaker J. Characterization of a second ligand binding site of the insulin receptor. Biochem Biophys Res Commun 2006;347:334:339.
38. Benyoucef S, Surinya KH, Hadaschik D, Siddle K. Characterization of insulin/IGF hybrid receptors: contributions of the insulin receptor L2 and Fn1 domains and the alternatively spliced exon 11 sequence to ligand binding and receptor activation. Biochem J 2007;403:603–613.
39. Smith BJ, Huang K, Kong G, Chan SJ, Nakagawa S, Menting JG, Hu SQ, Whittaker J, Steiner DF, Katsoyannis PG, Ward CW, Weiss MA, Lawrence MC. Structural resolution of a tandem hormone-binding element in the insulin receptor and its implications for design of peptide agonists. Proc Natl Acad Sci USA 2010;107: 6771–6776.
40. Derewenda U, Derewenda Z, Dodson EJ, Dodson GG, Bing X, Markussen J. X-ray analysis of the single chain B29-A1 peptide-linked insulin molecule. A completely inactive analogue. J Mol Biol 1991;220:425–433.
41. Hua QX, Shoelson SE, Kochoyan M, Weiss MA. Receptor-binding redefined by a structural switch in a mutant human insulin. Nature 1991;354:238–241.
42. Ludvigsen S, Olsen HB, Kaarsholm NC. A structural switch in a mutant insulin exposes key residues for receptor binding. J Mol Biol 1998;279:1–7.
43. Wan ZL, Huang K, Xu B, Hu SQ, Wang SH, Chu YC, Katsoyannis PG, Weiss MA. Diabetes-associated mutations in human insulin: crystal structure and photo-cross-linking studies of A-chain variant insulin Wakayama. Biochemistry 2005;44:5000–5016.
44. Jiracek J, Zakova L, Antolikova E, Watson CJ, Turkenburg JP, Dodson GG, Brzozowski AM. Implications for the active form of human insulin based on the structural convergence of highly active hormone analogues. Proc Natl Acad Sci USA 2010;107:1966–1970.
45. Lou M, Garrett TPJ, McKern NM, Hoyne PA, Epa VC, Bentley JD, Lovrecz GO, Cosgrove LJ, Frenkel MJ, Ward CW. The first three domains of the insulin receptor differ structurally from the insulin-like growth factor 1 receptor in the regions governing ligand specificity. Proc Natl Acad Sci USA 2006;103:12429–12434.
46. Vashisth H, Abrams CF. Docking of insulin to a structurally equilibrated insulin receptor ectodomain. Proteins 2010;78:1531–1543.

47. Vashisth H, Abrams CF. All-atom structural models for complexes of insulin-like growth factors IGF1 and IGF2 with their cognate receptor. J Mol Biol 2010;400:645–658.
48. De Meyts P. The structural basis of insulin and insulin-like growth factor-I receptor binding and negative co-operativity, and its relevance to mitogenic versus metabolic signalling. Diabetologia 1994;37 (suppl. 2):S135–S148.
49. Kiselyov VV, Versteyhe S, Gauguin L, De Meyts P. Harmonic oscillator model of the insulin and IGF1 receptors' allosteric binding and activation. Mol Syst Biol 2009;5:1–12.
50. Menting JG, Ward CW, Margetts MB, Lawrence MC. A thermodynamic study of ligand binding to the first three domains of the human insulin receptor: relationship between the receptor alpha-chain C-terminal peptide and the site-1 insulin mimetic peptides. Biochemistry 2009;48:5492–5500.
51. Abrams CF, Vanden-Eijnden E. Large-scale conformational sampling of proteins using temperature-accelerated molecular dynamics. Proc Natl Acad Sci USA 2010;107:4961–4966.
52. Maragliano L, Vanden-Eijnden E. A temperature accelerated method for sampling free energy and determining reaction pathways in rare events simulations. Chem Phys Lett 2006;426:168–175.
53. Maragliano L, Vanden-Eijnden E. Single-sweep methods for free energy calculations. J Chem Phys 2008;128:184110.
54. Maragliano L, Fischer A, Vanden-Eijnden E, Ciccotti G. String method in collective variables: minimum free energy paths and isocommittor surfaces. J Chem Phys 2006;125:024106.
55. Pillutla RC, Hsiao KC, Beasley JR, Brandt J, Ostergaard S, Hansen PH, Spetzler JC, Danielsen GM, Andersen AS, Brissette RE, Lennick M, Fletcher PW, Blume AJ, Schaffer L, Goldstein NI. Peptides identify the critical hotspots involved in the biological activation of the insulin receptor. J Biol Chem 2002;277:22590–22594.
56. Schaffer L, Brissette RE, Spetzler JC, Pillutla RC, Ostergaard S, Lennick M, Brandt J, Fletcher PW, Danielsen GM, Hsiao KC, Andersen AS, Dedova O, Ribel U, Hoeg-Jensen T, Hansen PH, Blume AJ, Markussen J, Goldstein NI. Assembly of high-affinity insulin receptor agonists and antagonists from peptide building blocks. Proc Natl Acad Sci USA 2003;100:4435–4439.
57. Vashisth H. Molecular simulation studies of the insulin receptor family. PhD thesis. Drexel University, PA. 2010.
58. Phillips JC, Braun R, Wang W, Gumbart J, Tajkhorshid E, Villa E, Chipot C, Skeel RD, Kalé L, Schulten K. Scalable molecular dynamics with NAMD. J Comput Chem 2005;26:1781–1802.
59. MacKerell, Jr, AD, Bashford D, Bellott M, Dunbrack, RL, Jr, Evanseck JD, Field MJ, Fischer S, Gao J, Guo H, Ha S, Joseph-McCarthy D, Kuchnir L, Kuczera K, Lau FTK, Mattos C, Michnick S, Ngo T, Nguyen DT, Prodhom B, Reiher WE, III, Roux B, Schlenkrich M, Smith JC, Stote R, Straub J, Watanabe M, Wiórkiewicz-Kuczera J, Yin D, Karplus M. All-atom empirical potential for molecular modeling and dynamics studies of proteins. J Phys Chem B 1998;102:3586–3616.
60. MacKerell ,AD, Jr, Feig M, Brooks CL, III. Extending the treatment of backbone energetics in protein force fields: limitations of gas-phase quantum mechanics in reproducing protein conformational distributions in molecular dynamics simulations. J Comput Chem 2004;25:1400–1415.
61. Humphrey W, Dalke A, Schulten K. VMD–visual molecular dynamics. J Mol Graph 1996;14:33–38.
62. Derewenda U, Derewenda Z, Dodson EJ, Dodson GG, Reynolds CD, Smith GD, Sparks C, Swenson D. Phenol stabilizes more helix in a new symmetrical zinc insulin hexamer. Nature 1989;338:594–596.
63. Xu B, Hu SQ, Chu YC, Huang K, Nakagawa SH, Katsoyannis PG, Weiss MA. Diabetes-associated mutations in insulin: consecutive residues in the B chain contact distinct domains of the insulin receptor. Biochemistry 2004;43:8356–8372.
64. Nakagawa SH, Tager HS. Role of the phenylalanine B25 side chain in directing insulin interaction with its receptor. J Biol Chem 1986;261:7332–7341.
65. Vashisth H, Maragliano L, Abrams CF. "DFG-flip" in the insulin receptor kinase is facilitated by a helical intermediate state of the activation loop. Biophys J 2012;102:1979–1987.
66. Vashisth H, Skiniotis G, Brooks ,CL, III. Using enhanced sampling and structural restraints to refine atomic structures into low-resolution electron microscopy maps. Structure 2012;20:1453–1462.
67. E W, Ren W, Vanden-Eijnden E. String method for the study of rare events. Phys Rev B 2002;66:052301.
68. E W, Ren W, Vanden-Eijnden E. Finite temperature string method for the study of rare events. J Phys Chem B 2005;109:6688–6693.
69. Ren W, Vanden-Eijnden E, Maragakis P, E W. Transition pathways in complex systems: application of the finite-temperature string method to the alanine dipeptide. J Chem Phys 2005;123:134109.
70. E W, Ren W, Vanden-Eijnden E. Simplified and improved string method for computing the minimum energy paths in barrier-crossing events. J Chem Phys 2007;126:164103.
71. Vanden-Eijnden E, Venturoli M. Revisiting the finite temperature string method for the calculation of reaction tubes and free energies. J Chem Phys 2009;130:194103.
72. Xu B, Huang K, Chu Y-C, Hu S-Q, Nakagawa S, Wang S, Wang R-Y, Whittaker J, Katsoyannis Panayotis G, Weiss MA. Decoding the cryptic active conformation of a protein by synthetic photoscanning: insulin inserts a detachable arm between receptor domains. J Biol Chem 2009;284:14597–14608.
73. Whittaker J, Whittaker LJ, Roberts, Jr, CT, Phillips NB, Ismail-Beigi F, Lawrence MC, Weiss MA. α-helical element at the hormone-binding surface of the insulin receptor functions as a signaling element to activate its tyrosine kinase. Proc Natl Acad Sci USA 2012;109:11166–71.
74. Huang K, Xu B, Hu SQ, Chu YC, Hua QX, Qu Y, Li B, Wang S, Wang RY, Nakagawa SH, Theede AM, Whittaker J, De Meyts P, Katsoyannis PG, Weiss MA. How insulin binds: the B-chain α-helix contacts the L1 β-helix of the insulin receptor. J Mol Biol 2004;341:529–550.
75. Glendorf T, Sorensen AR, Nishimura E, Pettersson I, Kjeldsen T. Importance of the solvent-exposed residues of the insulin B chain alpha-helix for receptor binding. Biochemistry 2008;47:4743–4751.
76. Chan SJ, Nakagawa S, Steiner DF. Complementation analysis demonstrates that insulin cross-links both α-subunits in a truncated insulin receptor dimer. J Biol Chem 2007;282:13754–13758.
77. Wan ZL, Xu B, Huang K, Chu YC, Li BR, Nakagawa SH, Qu Y, Hu SQ, Katsoyannis PG, Weiss MA. Enhancing the activity of insulin at the receptor interface: crystal structure and photo-cross-linking of a8 analogues. Biochemistry 2004;43:16119–16133.
78. Huang K, Chan SJ, Hua QX, Chu YC, Wang R, Klaproth B, Jia W, Whittaker J, De Meyts P, Nakagawa SH, Steiner DF, Katsoyannis PG, Weiss MA. The A-chain of insulin contacts the insert domain of the insulin receptor. J Biol Chem 2007;282:35337–35349.
79. Thorsoe KS, Schlein M, Steensgaard DB, Brandt J, Schluckebier G, Naver H. Kinetic evidence for the sequential association of insulin binding sites 1 and 2 to the insulin receptor and the influence of receptor isoform. Biochemistry 2010;49:6234–6246.
80. Nakagawa SH, Zhao M, Hua QX, Hu SQ, Wan ZL, Jia W, Weiss MA. Chiral mutagenesis of insulin. Foldability and function are inversely regulated by a stereospecific switch in the B chain. Biochemistry 2005;44:4984–4999.
81. Olsen HB, Ludvigsen S, Kaarsholm NC. The relationship between insulin bioactivity and structure in the NH2-terminal A-chain helix. J Mol Biol 1998;284:477–488.
82. Zhao M, Wan ZL, Whittaker L, Xu B, Phillips NB, Katsoyannis PG, Ismail-Beigi F, Whittaker J, Weiss MA. Design of an insulin analog with enhanced receptor binding selectivity: rationale,

structure, and therapeutic implications. J Biol Chem 2009;284:32178–32187.
83. Zakova L, Kazdova L, Hanclova I, Protivinska E, Sanda M, Budesinsky M, Jiracek J. Insulin analogues with modifications at position B26. Divergence of binding affinity and biological activity. Biochemistry 2008;47:5858–5868.
84. Rajpal G, Liu M, Zhang Y, Arvan P. Single-chain insulins as receptor agonists. Mol Endocrinol 2009;23:679–688.
85. Nakagawa SH, Hua QX, Hu SQ, Jia W, Wang S, Katsoyannis PG, Weiss MA. Chiral mutagenesis of insulin–contribution of the B20-B23 beta-turn to activity and stability. J Biol Chem 2006;281:22386–22396.
86. Hua QX, Xu B, Huang K, Hu SQ, Nakagawa S, Jia W, Wang S, Whittaker J, Katsoyannis PG, Weiss MA. Enhancing the activity of a protein by stereospecific unfolding: conformational life cycle of insulin and its evolutionary origins. J Biol Chem 2009;284:14586–14596.
87. Hua QX, Mayer JP, Jia W, Zhang J, Weiss MA. The folding nucleus of the insulin superfamily–a flexible peptide model foreshadows the native state. J Biol Chem 2006;281:28131–28142.
88. Hua QX, Nakagawa S, Hu SQ, Jia W, Wang S, Weiss MA. Toward the active conformation of insulin: stereospecific modulation of a structural switch in the b chain. J Biol Chem 2006;281:24900–24909.
89. Hua QX, Nakagawa SH, Jia W, Huang K, Phillips NB, Hu SQ, Weiss MA. Design of an active ultrastable single-chain insulin analog: synthesis, structure, and therapeutic implications. J Biol Chem 2008;283:14703–14716.
90. Hua QX, Ladbury JE, Weiss MA. Dynamics of a monomeric insulin analog: testing the molten-globule hypothesis. Biochemistry 1993;32:1433–1442.
91. Hua QX, Hu SQ, Frank BH, Jia WH, Chu YC, Wang SH, Burke GT, Katsoyannis PG, Weiss MA. Mapping the functional surface of insulin by design: structure and function of a novel a-chain analogue. J Mol Biol 1996;264:390–403.
92. Mirmira RG, Tager HS. Role of the phenylalanine B24 side chain in directing insulin interaction with its receptor. Importance of main chain conformation. J Biol Chem 1989;264:6349–6354.
93. Schäffer L. A model for insulin binding to the insulin receptor. Eur J Biochem 1994;221:1127–1132.
94. Mirmira RG, Nakagawa SH, Tager HS. Importance of the character and configuration of residues B24, B25, and B26 in insulin-receptor interactions. J Biol Chem 1991;266:1428–1436.
95. Mirmira RG, Tager HS. Disposition of the phenylalanine B25 side chain during insulin–receptor and insulin–insulin interactions. Biochemistry 1991;30:8222–8229.
96. De Meyts P. Insulin interactions with its receptors: experimental evidence for negative cooperativity. Biochem Biophys Res Comm 1973;55:154–161.
97. Sparrow LG, McKern NM, Gorman JJ, Strike PM, Robinson CP, Bentley JD, Ward CW. The disulfide bonds in the C-terminal domains of the human insulin receptor ectodomain. J Biol Chem 1997;272:29460–29467.
98. Schäffer L, Ljungqvist L. Identification of a disulfide bridge connecting the alpha-subunits of the extracellular domain of the insulin receptor. Biochem Biophys Res Comm 1992;189:650–653.
99. Whittaker J, Garcia P, Yu GQ, Mynarcik DC. Transmembrane domain interactions are necessary for negative cooperativity of the insulin-receptor. Mol Endocrinol 1994;8:1521–1526.
100. Bass J, Kurose T, Pashmforoush M, Steiner DF. Fusion of insulin receptor ectodomains to immunoglobulin constant domains reproduces high-affinity insulin binding *in vitro*. J Biol Chem 1996;271:
19367–19375.
101. Hoyne PA, Cosgrove LJ, Mckern NM, Bentley JD, Ivancic N, Elleman TC, Ward CW. High affinity insulin binding by soluble insulin receptor extracellular domain fused to a leucine zipper. FEBS Lett 2000;479:15–18.